Available online at www.sciencedirect.com

ScienceDirect

Procedia Structural Integrity 2 (2016) 1391–1404

Structural Integrity Procedia

www.elsevier.com/locate/procedia

21st European Conference on Fracture, ECF21, 20-24 June 2016, Catania, Italy

Fracture toughness determination by repetitive nano-impact testing in Cu/W nanomultilayers with length-scale-dependent films properties

E. Frutos[a]*, M. Karlik[b], T. Polcar[a,c]

[a] *Department of Control Engineering, Faculty of Electrical Engineering, Czech Technical University in Prague, Technická 2, Prague 6, Czech Republic.*

[b] *Department of Materials, Faculty of Nuclear Sciences and Physical Engineering, Czech Technical University in Prague, Trojanova 13, 120 00 Prague 2, Czech Republic.*

[c] *National Centre for Advanced Tribology (nCATS), University of Southampton, University Road, Southampton SO17 1BJ UK.*

Abstract

Nanoscale metallic multilayers based on Cu/W have been considered as a potential material for structural applications in nuclear reactors and for the cladding of storage tanks for advanced fuels kept at high temperatures. The understanding of how mechanical properties change in relation to periodicity, λ, is required in order to use Cu/W nano-multilayers as a protective coating against radiation damage. The aim of this work is to demonstrate the feasibility of using the repetitive-nano-impact technique to obtain quantitative fracture toughness, K_C, values in nano-multilayers and assess its variation as a function of λ.

Keywords: Dynamic fracture; Fracture toughness; Layered material; Impact testing; Stress intensity factor.

1. Introduction

Nanoscale metallic multilayers (NMMs) represent a new class of engineering materials consisting of alternating nanoscale multilayers of two different metals. These systems have been studied intensively during the last 10 years for many applications due to their exceptional mechanical properties. Examples of their unique properties are hardness enhancement (Misra et. al., 2005) and anomalous modulus compared with monolithic coatings of the constituent

* Corresponding author. Tel.: 00420 224357598. E-mail address: frutoemi@fel.cvut.cz

10.1016/j.prostr.2016.06.177

materials (Harms et. al., 2002) when the individual thickness layer, h, is less than 50 nm. Thereby, mechanical properties such as hardness and Young's modulus are related to the periodicity, λ, which is defined as the sum of each single layer, h_1+h_2 (typically $h_1=h_2$). The reason for these changes in the mechanical properties is related to the decrease in the length scale, as NMMs depart from the classic Hall-Petch relation (Misra et. al., 1998). Therefore, by combining metallic materials with high Young's modulus mismatch and different plastic behaviour, it is possible to design new NMMs with mechanical properties suitable for specific applications. For example, elevated strength (Hoagland et. al., 2002; Demkowicz et. al., 2007), superplasticity (Mukherjee, 2002), and high fatigue resistance (Wang et. al., 2006)are necessary in applications such as X-ray optics, thin film magnetic recording media, wear resistance coatings and microelectro-mechanical systems (MEMS) (Clemens et. al., 1999; Anderson et. al., 1999; Was et. al., 1996). However, perhaps the most useful property of these nano-multilayers is their substantially enhanced resistance to radiation damage when the thickness of their constituent layers is reduced below 5 nm (Mara et. al., 2007; Misra et. al., 2007).

Recently, Cu/W nano-multilayers have been considered as a potential material for structural applications in nuclear reactors and for cladding the tanks used for the storage of advanced fuels at high temperature (Mardon et. al., 1997; Suzuki et. al., 1994). This system is characterized by its high immiscibility due to the different crystal structures, *f.c.c (Cu)* vs. *b.c.c (W)*. An atomistic simulation has suggested that this type of incoherent interface is a good sink for radiation-generated point defects (Demkowicz et. al., 2008). This observation has also been supported by experiments, which showed that Cu/W multilayers (produced by magnetron sputtering) have a good He radiation tolerance (Gao 2011; Liu et. al., 2012). The combination of all these properties makes Cu/W nano-multilayers promising candidates for nuclear applications, since one of the major problems found within the inner parts of nuclear reactors is the appearance of cracks due to aging and embrittlement of materials exposed to radiation. Nevertheless, from the point of view of mechanical properties, these kinds of nano-coatings are not free of weaknesses.

One of the most important issues arises when the microstructure is subjected to continuous refinement (especially to the submicrometer scale) resulting in a progressive loss of plasticity (Meyers et. al., 2006; Zhang et. al., 2006). In fact, increasing attention is being paid to the dependence of length-scale-strength to plasticity/ductility of nanostructured metallic multilayers (Huang et. al., 2000; Mara et. al., 2008; Wen et. al., 2007). Zhu et. al. (2008) have also suggested that the fracture mode of is related to the strengthening mechanism, because crack propagation was arrested by the more ductile layers when the plastic strain is confined between thin nanolayers. Thereby, the limited plasticity of many NMMs is strongly dependent on the type of constituent layer, layer thickness and layer-to-layer interface/grain boundary. In the particular case of Cu/W i.e. ductile/brittle nano-multilayers, the understanding of how mechanical properties such as hardness, Young's modulus and fracture toughness, which is considered as one of the most important properties of structural materials, change in relation to λ are required in order to use it as a protective coating against irradiation at nuclear installation. Unfortunately, conventional methods used to determine the fracture toughness by single edge notched beam (SENB) (Damani et. al., 1996), chevron notched beam (CVNB) (Wan et. al., 2008) and double cantilever beam (DCB) (Whitney et. al., 1982), require complex experimental procedures and a minimum number of samples which have quite large dimensions, and therefore they are not applicable to coatings or thin layers. For this reason, nowadays there are great efforts being made in order to develop or improve techniques for obtaining mechanical properties from a very small volume, as is the case of coatings and thin nanolayers.

Impact techniques has recently been demonstrated that can be used for measuring fracture toughness in relatively thick intermetallic and ceramic coatings (~10 and ~4 μm, respectively) (Frutos et. al., 2013; Frutos et. al. 2016) and ceramic bulk materials (Frutos et. al., 2016). Depending on the number of impacts, it is possible to characterize the fracture toughness, as long as the magnitude of the initial energy is high enough to cause fracturing along the test. However, first it is necessary to ensure that the magnitude of the initial energy is high enough to produce a crack length whose dimensions are such that the indentation models can be used. To this end, the plastic region localized at the origin of the crack tip has to be very small so as not to affect the overall load deflection behaviour. In the case of coatings or thin layers, the use of this technique is limited by the fact that the load magnitude, P, and therefore the initial energy transmitted, $\varepsilon_{t,}$ has to be high enough to produce a crack. Nevertheless, the length of this crack has to be lower than 10% of the total coating thickness to avoid substrate contributions. For this reason, and in order to ensure a small plastic region localized at the origin of the crack tip, low P values (or small distance between the indenter tip

and the surface, S) have to be used. The use of cube-corner tips, with an angle of 35.3º, from Berkovich and Vickers tips, is more indicate because it is sharper. For a given load, the plastic strain rate underneath the tip is much larger than that for a Berkovich tip and, therefore, higher stresses can be produced for lower load values. Thereby, the proportionality between fracture toughness, K_C, and the ratio $P/c^{3/2}$ might be fulfilled, even for a load range from 1 to 5 mN. Therefore, classical indentation models (IM) proposed by Anstins et. al. (1981) and/or Laugier (1987) may be used for the calculation of K_C for coatings, as revealed in our previous work (Frutos et. al., 2013; 2016 and 2016).

The aim of this paper is to demonstrate the validity of the repetitive nano-impact technique for obtaining fracture toughness, K_C, values in thin Cu/W nano-multilayers and its variation as a function of λ. For this proposal, a proper knowledge of the crack morphology and its evolution with each new impact must be known, otherwise it is not possible to ascertain the most appropriate IM for the evaluation of K_C. If the ratio of $c/a \geq 3.5$, where c represents the crack length and a is the length from the centre of the projected area to the corner, the crack profile corresponds to a half-penny type, and the Anstin's model must be used. On the other hand, if the l/a ratio satisfies the condition: $1.1 \leq l/a \leq 2.5$, where l is the length from the corner of the indenter to the end of the crack, the crack profile corresponds to the Palmqvist type, and so the Laugier model must be used. Finally, fracture toughness calculation will be analysed and discussed in the framework of fracture toughness mechanics.

2. Experimental procedure

2.1 Materials

Three different Cu/W nanoscale metallic multilayer films (NMMs), with equal thickness ~1 μm, and with the individual layer thicknesses (i.e. one-half of the bilayer period) of 5, 15 and 30 nm were prepared. Depositions have been carried out, without any deliberate heating of the single crystal (100) Si wafer substrates, using a balanced magnetron sputtering system. Each DC source has been tilted by about 30º to the substrate (targets-to-substrate distance about 120 mm). The chamber was evacuated to a base pressure of 1×10^{-5} Pa. The depositions of Cu/W multilayers were carried out under partial pressure conditions, with an Ar gas flow of 10 sccm. The substrate holder was rotated at 10 rpm to obtain compositional homogeneity on the substrate. The power was kept constant at 110 W for copper and at 210 W for tungsten cathode during deposition, with corresponding deposition rates of 0.13 and 0.29 nm/s, respectively.

2.2 Microstructural characterization

Grazing X-ray diffraction (GIXRD) experiments have been carried out using an X'Pert-Pro Philips diffractometer with Cu Kα radiation. The grazing angle was set at 5º with a scan step size of 0.02º over an angle range of 2□=20-80º. Scanning transmission electron microscopy (STEM) observations have been performed using a FEI Tecnai G^2 F20 XT microscope with 200 KV accelerating voltages to observe the modulation structure and the interface structure.

2.3 Mechanical characterization

Mechanical properties were determined by nanoindentation experiments, using a Nanotest Advantage equipment from Micro Materials (Wrexham, UK). Nanoindentation was performed on the top surface of the NMMs by using a Berkovich tip with a load ranging between 1–5 mN. Loading and unloading times were fixed at 20 and 5 seconds in order to fix the strain rate at 0.05 and 0.2 s^{-1}, respectively. In all cases, the holding time was fixed at 15 seconds. Hardness (H) and Young's reduced modulus (E_R) were evaluated from the load-depth indentation curves using the Oliver and Pharr method (1992), by using the following equations:

$$H = \frac{P_{max}}{A_C} \quad (1)$$

$$\frac{1}{E_R} = \frac{1-\nu^2}{E_f} + \frac{1-\nu_i^2}{E_i} \quad (2)$$

In Eq. (1), P_{max} and A_C represent the maximum load and the projected contact area between the indenter and specimen

at maximum load, respectively. In Eq. (2), ν and ν_i, and E_f and E_i denote the Poisson's ratio and the Young's modulus for the film and the indenter, respectively. E_R refers to the reduced Young's modulus of the specimen determined according to Oliver and Pharr procedure. Young's modulus (E_i) and Poisson's coefficient (ν_i) of the diamond Berkovich tip are 1141 GPa and 0.07, respectively. Both hardness and Young's modulus results for a given load correspond to average values of at least 10 experiments.

The impact pendulum configuration of the Nanotest-Advantage was used for the cyclic impact testing solenoid connected to a timed relay was used to produce the repetitive impacts on the surface. A cube-corner diamond tip was accelerated from a distance, S, of 500 nm to the surface, producing an impact force, P, of 1 mN. The experiments were computer-controlled so that repetitive impacts occurred at the same position every 4 seconds over 300 seconds (75 impacts in total). The penetration depth was registered after every impact. Average values were obtained from at least 10 experiments performed in randomly selected areas on the surface of the coating.

3. Background and approaches

The plastic region localized ahead of the tip of an existing defect, i.e. at the origin of the crack tip, has to be very small so as not to affect the overall load-deflection response of cracked samples. Only then is it possible to assume a linear elastic fracture mechanism, and therefore classical indentation models can be used to calculate fracture toughness values. Selection of the most appropriate expression for evaluating K_C requires a proper knowledge of the crack morphology and its evolution with each new impact. If c/a≥3.5, the crack profile corresponds to a half-penny type and, therefore, the Anstins model is the most suitable for calculating the fracture toughness by using the expression:

$$K_{Ic} = \xi_\nu^R \left(\frac{E}{H}\right)^{1/2} \frac{P}{c^{3/2}}, \tag{3}$$

where P is the indentation load, c is the crack length, E is the Young's reduced modulus, H is the hardness and ξ_ν^R is the calibration coefficient, which depends on the tip and crack geometries. For half-penny cracks and for a cube-corner indenter geometry, this parameter is 0.040. On the other hand, if 1.1≤ l/a ≤ 2.5 or c/a≤3.5, the crack profile corresponds to the Palmqvist type, and therefore the Laugier model is the most suitable for calculating the fracture toughness from the expression:

$$K_{Ic} = \chi_\nu \left(\frac{a}{l}\right)^{1/2} \left(\frac{E}{H}\right)^{2/3} \frac{P}{c^{3/2}}, \tag{4}$$

where a and l are the lengths related to the half of the diagonal and the crack length from the apex of the footprint, respectively, while χ_ν is a constant similar to ξ_ν^R, for which the most indicative value for cube-corner geometry is 0.057.

4. Results and discussion

4.1 Microstructure characterization

Figure 1 shows scanning transmission electron microscopy high-angle annular dark field (STEM-HAADF) micrographs for λ=60. Although the layering structure is well defined in all cases, the layers, which are initially flat close to the coating/silicon interface, quickly develop a wavy character from the 2nd or 5th layer from the substrate interface to the top of the surface, depending of the periodicity (λ=10 and λ=60, respectively). This morphology results in the formation of large folds similar to a valley in both layers. In the case of W layers, the presence of disorder areas and large cavities is more than evident inside of the folds. As λ is reduced from 60 to 10, i.e., as the thickness of both layers is reduced, the Cu layers are no longer continuous. In fact, in some cases the successive W layers become interconnected. Furthermore, in the case of λ=10, these valleys give rise to the formation of channels with a high

percentage of amorphous areas and nanocrystals about 5nm.These channels extend perpendicularly from the top of the surface into the NMMs, along a dozen bilayers. More details of the multilayer structure can be found in our previous study (Monclus et. al., 2014).

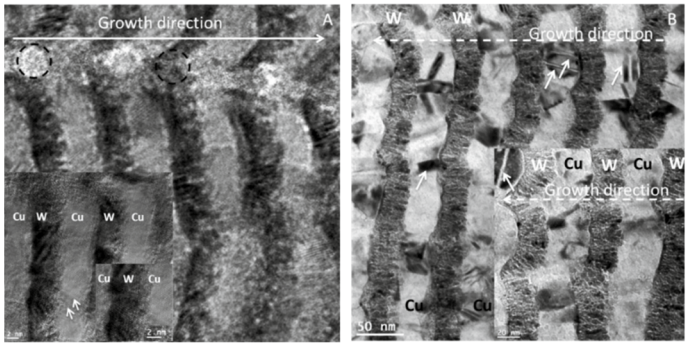

Fig.1. STEM–HAADF micrographs of the W/Cu nano-multilayers. The figures a) and b) show the higher grade of waviness in the W/Cu interfaces for λ=10, 1a) than for λ=60, 1b). The black circles show as the layers are not flat in λ=10 and neither are continuous because there are zones where Cu layers are connected and the same for W layers. Moreover, inserts in Fig. 1a) shows clear differences in the types of interfaces. Finally, insert in Fig. 1b) shows big grains in Cu layers with numerous growth twins, indicated by white arrows, and fine columnar grains in W layers.

X-ray diffraction (XRD) reveals a polycrystalline structure in each of the constituent layers, as it is shown in Fig. 2. For all λ studied, the layers composed of f.c.c. (Cu) and b.c.c. (W) crystals exhibit a strong (1 1 1) and (1 1 0) out-of-plane texture, respectively. Nevertheless, other less relevant textures were also found in the diffractograms. The most intense peaks show a shift with decreasing of λ, which suggested an evolution in the residual stresses. In the case of Cu, the peaks exhibit a significant shift toward lower 2θ angles with decreasing λ. Compared with the unstressed state (2θ=43.34º), this angle decreases from 43.33º to 43.13º as λ decreases from 60 to 10 nm. On the contrary, peak of W, is shifted toward lower 2θ angles with decreasing λ. Compared with the unstressed state (2θ=40.30º), this angle increases from 40.31º to 40.33º as λ decreases from 60 to 10. The lower the value of λ is, the smaller the compressive residual stresses in Cu layers and the higher the tensile residual stresses in W layers are. Moreover, a peak broadening observed for W (110) and particularly for Cu (111) textures with the decrease of λ suggest a larger amount of disorder at the interfaces of both layers. Such disorder might play a fundamental role in the accommodation of residual stresses of each layer and therefore affect the mechanical properties.

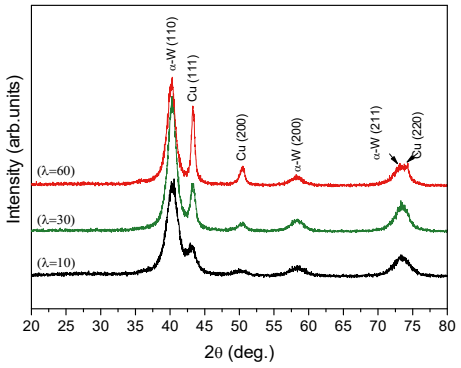

Fig.2. XRD diffractograms of the W/Cu nanomultilayers with the following periodicities. In red colour: λ=60 nm, green colour: λ=30 nm and blue colour λ=10 nm.

4.2 Mechanical characterization

Figure 3 shows the variation of the Young's reduced modulus as a function of the maximum indentation depth, *h*,

and coating thickness, *t*, ratio. The increased scatter at low depths (h/t < 0.1) is due to tip rounding and surface roughness effects. Nevertheless, a strong dependence of the maximum depth on λ is evident. For λ=60, the Young's modulus gradient is around 34% between depths 70 and 130 nm, whereas for the lowest periodicity (λ=10) the gradient is much lower, around 16%. On the other hand, Young's reduced modulus reaches a plateau with different values depending on the periodicity. In the case of λ=10, this value is ~ 167 GPa; in contrast, for medium and high λ, the modulus decreases after reaching a maximum value of ~ 183 GPa.

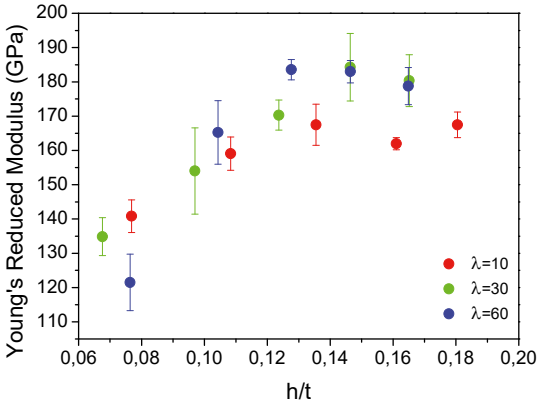

Fig.3. Young's reduced modulus as a function of ratio between the maximum indentation depth, h, and the total layer thickness, t, for the three λ studied in W/Cu nano-multilayers.

Such a decrease is due to the plastic deformation of the substrate. Thus, the greater the mismatch between the Young's modulus values of the layers (E_W≈395 GPa and E_{Cu}≈120 GPa) and the substrate (E_{Si}≈130 GPa), the greater the substrate effect is. Thereby, substrate contribution must be taken into account (removed). Table 1 shows the true Young's modulus in the nano-multilayers, E_f, for the three periodicities studied. It is clear that these values do not follow the inverse rule of mixture between W and Cu layers that should render a value of E≈250 GPa. The true Young's modulus increases from 183 GPa (λ=60) to 198 GPa (λ=30) and then drops to 166 GPa (λ=10). This drop with λ may be explained by the presence of partially amorphous-like W/Cu interfaces, as detailed above. Thereby, for λ=10, the relative ratio of such a disordered interface is the highest, resulting in a lower true Young's modulus. Furthermore, this may be consistent with the broadening of XRD peaks with decreasing periodicity. Nevertheless, these changes in the values of Young's modulus remain controversial, as there is no clear explication of their origin or magnitude.

Figure 4 shows the Berkovich hardness profiles as a function of the h/t. For λ= 10, the hardness profile reaches a saturation value of about 6 GPa for a depth between 100-180 nm. On the contrary, for the cases of λ=30 and λ=60, the hardness profile is not stabilized due to substrate effect. Nevertheless, from the true Young's modulus values (obtained for each periodicity by Eq. 3 and using the Eq. 4; Frutos et. al., 2015) it is possible to calculate the true Berkovich hardness values without substrate effect, H_f, for every load. True hardness values, H_f, for Cu/W nano-multilayers correlate to the plateaus in the measured hardness values (Fig. 5). Table 1 shows the H_f obtained for the three periodicities studied, where a similar trend as for the E_f is observed. Hardness shows an increase as λ is reduced from λ=60 to λ=30, increasing from 6.7 to 7.3 GPa, while it exhibited a decrease to 5.2 GPa for λ=10. Once this true Berkovich hardness value is known, it is also possible to study the effect of periodicity on the flow stress.

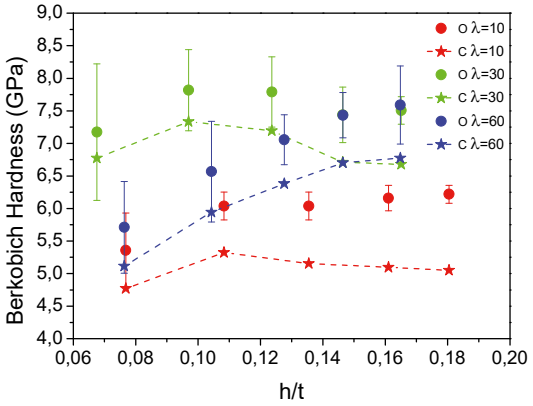

Fig.4. Directly Berkovich hardness values from nanoindentation test (O) and true Berkovich hardness values calculated (C) as a function of the ration between maximum depth, h, and the total layer thickness, t, for the three λ studied in W/Cu nano-multilayers.

A useful way to correlate the elastic-plastic transition (and therefore the flow stress to the plastic strain) during nanoindentation experiments is through the yield strength value. The yield strength value is directly related to the hardness through: $H \approx 2.7\sigma_y$, which is obtained from the slip line field theory of Tabor (1951). Having calculated the yield strength via the aforementioned relation, it is possible to observe the trend of the flow stress. As can be seen in table 1, $\sigma_{2.7}$ increases from 2.48 to 2.70 GPa for λ decreasing from 60 to 30, while it decreased to 1.93 GPa in the case of λ=10. In this regime, flow stress, and therefore the plastic deformation, is related to modulus mismatch between both constituent layers (Koehler, 1970), as well as the misfit dislocations/interface interaction (Rao et. Al., 2000). Thereby, plastic deformation is located primarily in the soft/ductile layer and it is transmitted through elastic deformation of the hard/brittle layer. At the nanoscale, this deformation is mainly controlled by the nucleation and motion of a single dislocation, rather than dislocation pileups in the soft and ductile phase. Since only a single dislocation is transmitted through the hard and brittle layer, the yield strength of the multilayer takes place. This strain mechanism is known as confined layer slip (CLS) in which the glide of a single dislocation loop in the soft phase (bounded by two interfaces) comes into operation (Phillips et. al., 2003). On the other hand, in this regime, it has also been postulated that factors such as large modulus mismatch (or Koehler stress), large strain mismatch, or high enthalpy of formation are usually considered favorable for hardness enhancement (Li et. al., 2007). In the particular case of Cu/W multilayers, the higher the yield strength mismatch is, the lower the number of brittle/hard plastically deformed layers. Thereby, the plastic deformation, contained in the Cu layers, is transmitted elastically through a higher number of W layers. The peak in hardness and/or yield strength may suggest the transition of deformation mechanism, where single dislocations cross the interface instead of slipping in the confined layer.

According to the CLS model, the applied stress, σ_{CLS}, required to propagate a glide dislocation loop confined to one Cu layer, is given by:

$$\sigma_{CLS} = M\frac{\mu^* b}{8\pi h'}\left(\frac{4-\nu}{1-\nu}\right) ln\frac{\alpha h'}{b} - \frac{f}{h} + \frac{\mu^* b}{L(1-\nu)}, \quad (5)$$

where M is the Taylor factor; $h' = h_{Cu}/sin\varphi$ is the layer thickness parallel to the glide plane; φ is the angle between the slip plane and the interface; b is the absolute length of the burgers vector; ν is the Poisson ratio of Cu; $\mu^* = \frac{\mu_W \mu_{Cu}}{2(V_W \mu_{Cu} + V_{Cu}\mu_W)}$ is the mean shear modulus of the Cu/W multilayer (which can be estimated by shear modulus μ_{Cu}, μ_W and volume fraction V_{Cu}, V_W of the Cu and W layers); α represents the core cut-off parameter, which varies from 0.2 to 1 depending on whether the dislocation has a compact core or spread core; f is the characteristic interface stress of the multilayer and its value for metallic materials is between 2-3 Jm^{-2} (Cammarata, et al., 2000); L is the mean spacing of glide loops in a parallel array ($L = bm/\varepsilon V_x$ (Embury et. al., 1994)); V_x is the volume fraction of the X layer, Cu, that is directly related to the individual thickness layer ratio: η (i.e. $V_x = \eta/(1+\eta)$), defined as h_W/h_{Cu} ($h_W=h_{Cu}$, η=1); ε is the in-plane plastic strain; and m is a strain resolution factor of the order of 0.45 for the active slip systems in bcc

crystals structures. Tensile data on nanoscale metallic multilayers (Han et. al., 2009) show a low work-hardening rate after the initial 1-2% plastic strain. Following this treatment, the initial value chosen for ε is 2%, which is then used to calculate the yield strength of Cu/W multilayers as per Eq. 5. The values of the parameters used are as follows: M=3.06, $\mu_{Cu} = 48.3$ GPa, $\mu_W = 161$ GPa, ν=0.343, b = 0.2556 nm, α=0.2 (compact core) and 1 (spread core), f =3 Jm^{-2} and φ = 70.5º. Table 1 shows the yield strength values (obtained using Eq. 5) for the extreme values of core cut-off and the experimentally measured yield strength values, $\sigma_{2.7}$. For the first case, α=1, σ_{CLS} values increase continuously as λ decreases from 60 to 10. Thereby, σ_{CLS} values for λ=60, λ=30 and λ=10 are 2.13, 2.73 and 4.34 GPa, respectively. These values are in good agreement with the $\sigma_{2.7}$ values for λ=60 and λ=30. However, in the case of λ=10, the σ_{CLS} value is extremely high and it is not compatible with the $\sigma_{2.7}$ value obtained above. In contrast, for the second case, α = 0.2, σ_{CLS} values continuously grow as λ is reduced, therefore cannot be compared with the values obtained via direct measurement. These values are 1.81, 2.08 and 2.38 GPa for λ=60, λ=30 and λ=10, respectively. However, if the calculation of σ_{CLS} is repeated with an in-plane plastic strain, ε, value of 1%, it can be seen that σ_{CLS} values grow from 1.18 GPa, for λ=60, to 1.76 GPa, for λ=10. It is evident that for the highest and intermediate values of λ, the correct core cut-off value used for the calculation of the yield strength through confined layer slip system has to be α=1. However, for the lowest λ, its $\sigma_{2.7}$ value is only compatible with a σ_{CLS} value obtained from of a core cut-off of α=0.2 and an in-plane plastic strain of ε=1%. In any case, for the three values of λ studied, $\sigma_{2.7}$ values can be explained only through the CLS model. Therefore, the saturation value reached in the yield strength for λ=30, and its subsequent decrease for λ=10, is not a consequence of a change in the strain mechanism from CLS to IBS model, such as others NMMs have shown (Lai et. al., 2007; Zhang et. al., 2012). Nevertheless, this decrease in the yield strength value shows a change in the trend of the crack propagation, and therefore in its fracture toughness behaviour.

Table 1.Values of true Young's modulus, E_f, and Berkovich hardness H_f, as well yield strength values (obtained using Eq. 7) for the extreme values of core cut-off and the experimentally measured yield strength values, $\sigma_{2.7}$, obtained for the three periodicities studied.

λ (nm)	H_f (GPa)	E_f (GPa)	$\sigma_{2.7}$ (GPa)	σ_{CLS} $\alpha = 1$ $\varepsilon = 2\%$ (GPa)	σ_{CLS} $\alpha = 0.2$ $\varepsilon = 2\%$ (GPa)	σ_{CLS} $\alpha = 0.2$ $\varepsilon = 1\%$ (GPa)
10	5.24	166	1.93	4.34	2.38	1.76
30	7.27	198	2.70	2.73	2.08	---
60	6.74	183	2.48	2.13	1.81	1.18

4.3 Nano-repetitive-impact testing

As has been revealed in ours previous works, depending on the indenter geometry, the ductility of the material and the magnitude of the initial ε_t, the maximum strength may be reached at the first impact. From the first impact, which is actually a high strain rate indentation, it is possible to produce a notch with the same shape as the cube-corner indenter, whose purpose is to concentrate the maximum possible stress around the impact point just underneath the apex of this notch. Therefore, if initial ε_t is high enough to match the material yield strength, and the capacity of the material for the accumulation of plastic deformation is negligible, the hypothetical crack (nucleated in the first impact) will be propagated from the apex of the notch throughout successive impacts. From the graphical point of view, this crack propagation is equivalent to the opening of the material surface around the indenter, as the successive increase in the impact depth (accumulated with each new impact) is similar to the length travelled by the crack. This would be reflected in big decreases in the initial growth rate of the depth, $\dot{h}$, along the curve of the accumulative impact depth, h, as a function of the impacts number (Fig. 5). It is important to remark that all h values shown in this figure have been obtained by subtracting the depth reached at the first impact, h_1, since it is actually a normal indentation done at high strain rate. During this indentation, a cube-corner shape notch is created, and the plastic strain (200 %) is accumulated in a small volume underneath the apex of the footprint. The abrupt growth in the impact depth reached between the first and the second impact suggests that the crack is nucleated, progressing quickly with the successive impacts. This is attributed as a continuous opening of the surface around the cube-corner indenter. After a certain

number of impacts, initially high $\dot{h}$ values approach zero, and the crack tip becomes increasingly blunt - a consequence of the energy necessary to create the new surface being equal to the plastic strain energy, as postulated by Griffith. Thereby, a plateau is reached in which not a change in the impact depth, h, is, subjecting the surface to a fatigue process.

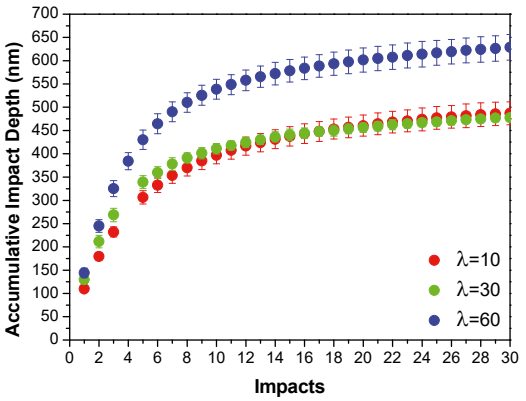

Fig.5. Increase in the accumulative impact depth, h, as a function of the impact number for the three λ.

4.4 Fracture toughness

From the nano-repetitive impact test it is possible to obtain different mechanical properties, as has been highlighted in previous work [48, 49]. However, the most representative of them is the fracture toughness, K_{Ic}, whose value is not unique, since the magnitude of the strain rate, $\dot{\epsilon}$, is not constant. Therefore, it should take into consideration that as the number of impacts increases, $\dot{\epsilon}$ progressively decreases, as $\dot{h}$ decreases and h increases with each new impact - the net effect being that the initial energy transmitted (ε_t=0.5 nJ) does not remain constant throughout all impacts. Therefore, the first priority is to check if impacts performed with a low initial ε_t value are able to develop a crack under strain plane conditions. Thereby, it is fundamental that we calculate the evolution of both ratios (h/a and l/a) in order to be sure that classical indentation model (Anstins and/or Laugier) can be used, and which of them is the most appropriated for calculating the fracture toughness. For this purpose, it is necessary to calculate (with each new impact) the evolution of a, which is the length from the centre of the projected area to the corner, and l, which is the length from the corner of the indenter to the end of the crack. The procedure of how to calculate these parameters has been published recently in ours previous works.

Figure 6 shows the evolution of the h/a ratio as a function of the impacts for the three values of λ studied. For λ=60 (Blue triangles) it can be seen that the h/a ratio values are above 3.5 from the first impact, and therefore it is possible use the IM proposed by Anstins (Eq. 3). By contrast, for λ=30 and λ=10 (Green and red triangles, respectively) it is not possible use this IM until the fifth impact, with the IM proposed by Laugier (Eq. 4) preferable for the first four impacts. Nevertheless, we will use directly the Anstins IM, without loss of generality, since the surface is opening to a greater degree with each new impact, and the material slides around the lateral surface while the initial $\dot{\epsilon}$ decrease until achieves quasi-static conditions. This way of breaking the surface is similar to half-penny crack morphology, since the hypothetical crack origin is located in the apex of the footprint, i.e., in the vertex of the initial notch, which acts as a stress concentrator. Crack growth from this point will produce morphology similar to a halpenny-crack. Thereby, from Anstins formulation and knowing the true Young modulus, E_f, obtained from conventional nano-indentation tests, the dynamic hardness values, H_d, and the crack length, h, for each new impact, it is possible to calculate the fracture toughness, Kc. Figure 7 shows the K_{IC} evolution obtained from H_d values for the three λ studied and with $\xi_\nu^R = 0.040$. The trend in K_{IC} values as a function of the number of the impacts exhibits similar behaviour, decreasing until reaching a constant value. The K_{IC} values for the first impact, K_{Ic}^1, and the value achieved on the plateau, K_{Ic}^P, are: 2.39 MPa$\sqrt{m}$, for λ=10, 3.00 MPa$\sqrt{m}$, for λ=30, 2.85 MPa$\sqrt{m}$, for λ=60 and 1.60 MPa$\sqrt{m}$,

for λ=10, 1.90 MPa$\sqrt{m}$, for λ=30, 1.77 MPa$\sqrt{m}$, for λ=60, respectively. On the other hand, whereas in the Anstins formulation (Eq. 5) in which the ratio between the hardness and Young's modulus is implicit, another possibility for the calculation of K_{IC} makes use of the only one true Berkovich hardness value, H_f, instead of the H_d values. For comparison, figure 7 also shows the evolution in fracture toughness values, replacing in Eq. 5 the H_d values for the constant true H_f value. In this figure it can be seen that the ${}^*K_{Ic}^1$ values, obtained using H_f, are extremely high and do not correspond with real ones. As in the previous case, fracture toughness values evolve until reaching the same plateau. Initial ${}^*K_{Ic}^1$ and ${}^*K_{Ic}^P$ values are shown in the table 2 for the three λ studied. Therefore, the use of the true Berkovich hardness is not recommended because its constant value does not reflect the evolution of hardness, as a consequence of the strain rate evolution. Nevertheless, these fracture toughness values also show that the strain rate drops from a value ~10^3 s^{-1} to achieve the quasi-static conditions (10^{-3} s^{-1}); this being point at which both hardness values, dynamic and true Berkovich, are coincident.

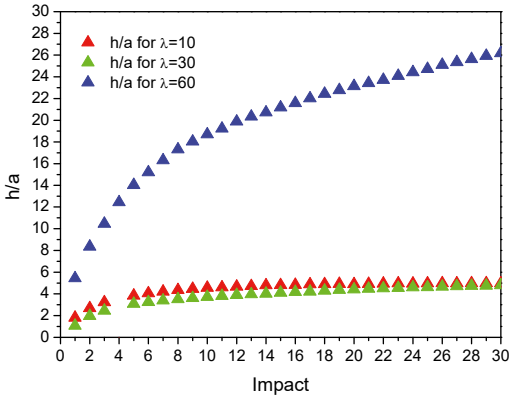

Fig. 6. Evolution of the h/a ratio as a function of the impacts for the three λ studied.

5. Discussion

As it is well known, the ductility is expected to vary with the yield strength, since when yield strength is increased, the strain necessary to achieve the critical stress for fracture decreases. Thereby, an increase in yield strength would be expected to produce a proportional decrease in ductility, provided that the strength is achieved with the same microstructure. This behaviour typically happens in NMMs, since the strain resistance changes when the thickness layer of the ductile phase is reduced. This indicates that the strengthening via interface constraint will sacrifice deformability remarkably, because the movement of dislocations will be strongly suppressed by the increased interfaces. Therefore, the number of interfaces is the predominant factor controlling the deformation and fracture in multilayer films.

In the particular case of Cu/W multilayers, when the thickness of the Cu layer is reduced from 30 (λ=60) to 15 nm (λ=30), the yield strength ($\sigma_{2.7}$) increases from 2.48 to 2.70 GPa. This strengthening via interface constraint sacrifices deformability significantly and, therefore, movement of dislocations is strongly supressed by the increased number of interfaces, producing Cu nanolayers with a higher brittle behaviour than occurs in W nanolayers. However, when Cu layer thicknesses are reduced to 5 nm, a decrease in the yield strength (to 1.93 GPa) is observed. This is a consequence of the amorphous region (~2 nm), which becomes especially important when it is close to 50 % of the layer thickness. Thereby, the presence of these amorphous areas produces a decrease in the in-plane plastic strain, ε, from 2 to 1%, and because of that the dislocations have a more compact core cut-off (α=0.2). As such, the presence of these amorphous regions produces a decrease in the yield strength value and therefore changes in the crack propagation.

Crack nucleation and propagation in Cu/W multilayers primarily takes places in the brittle W layer, and further propagation of the cracks will be suppressed by the surrounding ductile Cu layers, resulting in crack arrest. The plastic strain capability of Cu layers is heavily dependent on the dislocation movement. In the CLS region, a few dislocations

in the Cu layers are movable and, therefore, these have some deformation capability to shield the propagation of tiny cracks. For thinner crack sizes or h_W, there is a higher probability for the Cu layers to arrest the cracks. However, beyond the CLS region, the NMMs can be equivalent to composites consisting of alternate brittle Cu layers and brittle W layers. Here, a larger number of interfaces contribute more to worsening the deformability and, therefore, the ductility and fracture toughness.

Table 2. Fracture toughness values calculated in the first impact and the value achieved in the plateau for the different proposed routes as a function of the periodicity, λ. Thereby, K_{Ic} values, are compared values obtained from classical framework of fracture toughness mechanics.

λ (nm)	$\boldsymbol{K_{Ic}^{1}}$ (MPa$\sqrt{\boldsymbol{m}}$)	$\boldsymbol{K_{Ic}^{P}}$ (MPa$\sqrt{\boldsymbol{m}}$)	$\boldsymbol{{}^{*}K_{Ic}^{1}}$ (MPa$\sqrt{\boldsymbol{m}}$)	$\boldsymbol{{}^{*}K_{Ic}^{P}}$ (MPa$\sqrt{\boldsymbol{m}}$)	$\boldsymbol{K_{Ic}}$ (MPa$\sqrt{\boldsymbol{m}}$)
10	2.39	1.60	5.29	1.62	1.62
30	3.00	1.90	7.50	1.93	1.97
60	2.85	1.77	7.26	1.75	1.82

The degree of accuracy of fracture toughness values calculated above from a crack, which has been induced by repetitive-nano-impact tests, using the classic Anstins indentation model and two different approaches for calculating the crack length from which the nano-multilayer suffers a brittle fracture, can be analysed in the framework of fracture toughness mechanics (Beuth, 1992). In this framework, fracture of brittle films can be described analytically by 2-D steady-state models (Beuth, 1992), in which the steady-state energy release rate, ξ, is a parameter only dependent on the shape of the crack tip and maintained as the crack propagates. Thus, ξ depends of the crack size, which can be expressed as:

$$\xi = \frac{\sigma_y^2 * h_T}{E_{fR}} * g(\alpha, \beta), \tag{6}$$

where E_{fR} is the Young's reduced modulus of the NMMs; σ_y is the tensile stress of NMMs at ε; h_T is the total nano-multilayer thickness; and $g(\alpha, \beta)$ is a dimensionless quantity parameter that can be calculated from the elastic mismatch between the film and substrate with α and β being the two Dundurs' parameters (Dundurs et. al., 1969) characterizing the elastic mismatch between film and substrate. For a crack tip in the nano-multilayer, Beuth has shown that $g(\alpha, \beta)$ is given by:

$$g(\alpha, \beta) = 3.951 * \eta_f * \left(1 - \eta_f\right)^{1-2s} * \left(1 + \lambda_1 * \eta_f\right)^2, \tag{7}$$

where $\eta_f = \frac{a_f}{h_T}$ (a_f is the length crack perpendicular to the nano-multilayer/substrate interface and h_T is the total thickness of the nano-multilayer ~1 μm) and s (0.4696) and λ_1 (-0.01792) are a fitting parameter to the full numerical solution (Table 2) from Ref. (Suo et. al., 1992). For a Cu/W NMMs, i.e. a ductile/brittle nano-multilayer, the value of α is ≈-0.17, β is equal to α/4, and the value of λ_1 has been estimated (through linear interpolation) according to Ref. (Beuth, 1992). On the other hand, the a_f value has been estimated from the value of $\left(\sqrt{2} * (h\_2 - \Delta h)\right)$, for which of dynamic hardness value, H_d, is coincident with the true Berkovich hardness value, H_f. Once these values are known, together with the above experimental data (True Young's modulus of the nano-multilayer, E_f, and the yield strength value, $\sigma_{2.7}$), the fracture toughness (K_{Ic}) of the Cu/W NMMs can be calculated through the expression:

$$K_{Ic} = \sqrt{\frac{E_f * \xi}{(1 - \nu^2)}}, \tag{8}$$

where ν is the Poisson's ratio of NMMs, whose value of 0.3115 has been calculated according to the rules of mixtures (ROM). The K_{Ic} values, for the three Cu/W NMMs, as a function of h_{Cu} (and therefore as a function of λ) are compared

with the above values obtained from the two different methods and collected in the table 2. As can be seen, these new K_{Ic} values obtained from classical framework of fracture toughness mechanics for the three values of λ studied show a similar trend, and they can be compared with the previous values in table 2. Thus, fracture toughness values increase from 1.82 MPa$\sqrt{m}$ to 1.97 MPa$\sqrt{m}$ when λ is reduced from 60 to 30, and then descend to 1.62 MPa$\sqrt{m}$ for λ=10.

As was pointed out previously, regardless of λ, W morphology layers are composed of columnar grains. However, these kinds of grain boundaries are not always strong. If the layer interface is sufficiently strong, fractures tend to initiate first within the stiff layer as long as the cohesive strength of these columnar grain boundaries are comparatively weak. Therefore, W columnar grain boundaries become natural sources of cracking. On the other hand, its weakness increases as a consequence of the amorphous regions, thus the Cu nanolayer becomes the only link bridging the cracks in the W nanolayer. Due to stress concentration, and a loss of the interface barrier at the crack tip, the Cu nanolayer is easily deformed via dislocation gliding. Therefore, deformation of the Cu layers is confined to local areas that, with decreasing λ, allow the formation of grain-sized steps and cavities at the fracture surface, which reduce the fracture toughness values, as is the case for λ=10.

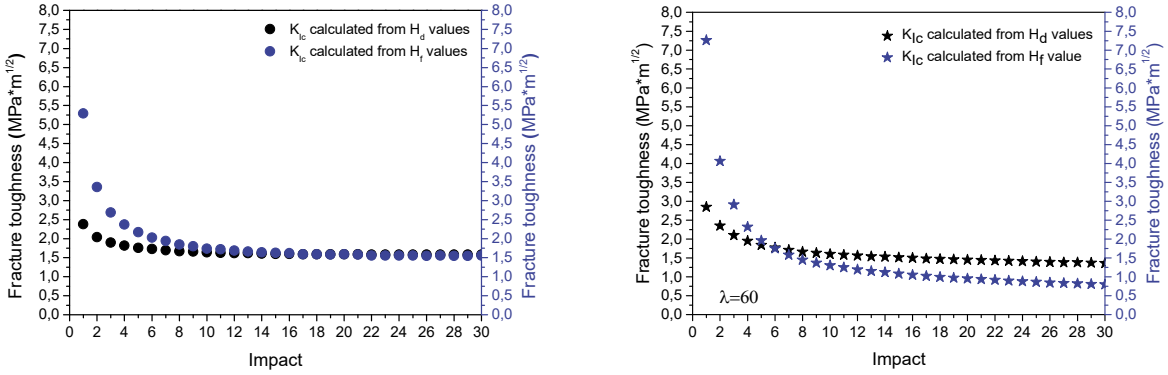

Fig. 7. Shows the K_{IC} evolution obtained from H_d (Black colour) and H_f (Navy blue colour) for λ=10 and λ=60 studied and with ξ_v^R = 0.040.

6. Conclusion

Mechanical properties (Young's modulus, Berkovich hardness, flow stress and fracture toughness) of metallic W/Cu nano-multilayers with different λ, deposited by magnetron sputtering, have been investigated through different instrumented indentation (Nanoindentation and repetitive nano-impact). Present results clearly show that the effect of the substrate must be removed in the case of thin NMMs (~1 μm), even when indentations have been done below 10% of total coating thickness. Only then is it possible to obtain the true values of hardness, H_f, and Young's modulus, E_f, and study its dependence with the periodicity, λ, and microstructure. Both values show dependencies, not only on the thickness of each layer (h_{Cu} and h_W), i.e., with λ, but also with the ductile or brittle nature of each layer, as well as on the microstructure type: crystalline/sharp or amorphous/disorder, which are developed depending on the interface type: Cu/W and W/Cu, respectively. Thus, H_f and E_f do not reach their maximum values for λ=10, as would be expected for layers with thicknesses below 50 nm (where CLS theory is applicable) and therefore the higher the number of interfaces and the out-of-plane compression stress, the greater the hardness and modulus are, respectively. Rather, maximum values are achieved for λ=30, because when the layer thickness is reduced to 5 nm, i.e., λ=10, the disorder percent can reach 75% of the thickness, reducing the hardness and modulus values.

On the other hand, it is shown as repetitive-nano-impact tests is a strong and versatile tool to obtain quantitative fracture toughness values in thin W/Cu nano-multilayers. Because the nucleation of a single crack and its propagation, along the perpendicular direction to the interfaces, takes place with each new impact. For this, sharp indenter geometry, like cube-corner, and an appropriate initial ε_t value must be selected in order to not to produce crack lengths

higher than 10% of the total thickness. Crack length can be measured with each new impact and therefore the correct indentation model for calculating fracture toughness can be selected. This allows studying the evolution of h/a or l/a ratios, as a function of the impacts, i.e. the crack geometry, which evolves from Palmqvist crack (Laugier IM) to half-penny crack (Anstins IM). Consequently, it is possible to study the proper evolution of the different values of fracture toughness as a function of different λ. Fracture toughness values obtained for W/Cu nano-multilayers, from Anstins indentation model, show an increase from 1.77 $MPa\sqrt{m}$ to 1.90 $MPa\sqrt{m}$ when the periodicity, λ, is reduced from 60 to 30 nm and finally, a decrease until 1.77 $MPa\sqrt{m}$ for λ=10 nm.

Finally, degree of accuracy of fracture toughness values, calculated from a crack induced by repetitive nano-impact tests, using the classic Anstins indentation model has been compared in the framework of fracture toughness mechanics, getting three new K_{Ic} values for these three λ. Thus, fracture toughness values increase from 1.82 $MPa\sqrt{m}$ to 1.97 $MPa\sqrt{m}$ *when* λ is reduced from 60 to 30 nm, and then descend to 1.62 $MPa\sqrt{m}$ for λ=10 nm. These values are to identical to those reported above, which demonstrates that proposed methods are useful to calculate quantitative fracture toughness values in thin nano-multilayers.

Acknowledgements
The authors wish to express their thanks for the financial support of the European Commission through the project RADINTERFACES (Grant Agreement Number 263273) and the Czech Science Foundation through the project 14-32801P.

References

Anderson, P. M., Foecke, T., Hazzledine, P. M., 1999. Dislocation-Based Deformation Mechanisms in Metallic Nanolaminates. MRS Bull. 27, 27-33.
Anstis, G. R., Chantikul, P., Lawn B. R., Marshall D. B., 1981. A Critical Evaluation of Indentation Techniques for Measuring Fracture Toughness: I, Direct Crack Measurements. J. Am. Ceram. Soc. 64, 533-538.
Banerjee, R., Thompson, G. R., Anderson, P. M., Fraser, H. L., 2003. Sputter deposited nanocrystalline Ni-25Al alloy thin films and Ni/Ni_3Al multilayers. Thin Solid Films. 424, 93-98.
Beuth, J. L., 1992. Cracking of thin bonded films in residual tension Jr. Int J Solids Struct. 29, 1657-1675.
Cammarata, R. C., Sieradzki, K., Spaepen, F., 2000. Simple model for interface stresses with application to misfit dislocation generation in epitaxial thin films. J. Appl. Phys. 87, 1227.
Clemens, B. M., Kung, H., Barnett, S. A., 1999. Structure and Strength of Multilayers. MRS Bull. 24, 20-26.
Damani, R., Gstrein, R., and Danzer, R., 1996. Critical Notch-Root Radius effect in SENB-S Fracture Toughness Testing. J. Eur. Ceram. Soc. 16, 695-702.
Demkowicz, M. J., Argon, A. S., Farkas, D., Frary, M., 2007. Simulation of plasticity in nanocrystalline silicon. Philos. Mag. 87, 4253-4271.
Demkowicz, M. J., Hoagland, R. G., Hirth, J. P., 2998. Interface Structure and Radiation Damage Resistance in Cu-Nb Multilayer Nanocomposites. Phys. Rev. Lett. 100, 136102.
Donohue, A., Spaepen, F., Hoagland, R. G., Misra, A., 2007. Suppression of the shear band instability during plastic flow of nanometer-scale confined metallic glasses. Appl. Phys. Lett. 91, 241905.
Dundurs, J., Bogy, D., B., 1969. Edge-Bonded Dissimilar Orthogonal Elastic Wedges Under Normal and Shear Loading. J. Appl. Mech. 36, 650-652.
Embury, J., D., Hirth, J., P., 1994. On dislocation storage and the mechanical response of fine scale microstructures. Acta Metall. Mater. 42, 2051-2056.
Frutos, E., González-Carrasco, J., L., 2013. A method to assess the fracture toughness of intermetallic coatings by ultramicroindentation techniques: Applicability to coated medical stainless steel. Acta Mater. 61(6), 1886–1894.
Frutos, E., González-Carrasco, J., L., Polcar, T., 2016. Nanomechanical characterization of alumina coatings grown on FeCrAl alloy by thermal oxidation. J. Mech. Behav. Biomed. Mater. 57, 310-320.
Frutos, E., González-Carrasco, J., L., Polcar, T., 2016. Repetitive nano-impact tests as a new tool to measure fracture toughness in brittle materials. J. Eur. Ceram. Soc. (In press).
Gao, Y., 2011. Radiation tolerance of Cu/W multilayered nanocomposites. *Radiation tolerance* of *Cu/W multilayered nanocomposites.* J.Nucl.Mater. 413, 11-15.
Han, S., M., Phillips, M., A., Nix, W., D., 2009. Study of strain softening behavior of Al–Al_3Sc multilayers using microcompression testing. Acta Mater. 57, 4473-4490.
Harms, U., Schwarz, R., B., 2002. Anomalous modulus and work function at the interfaces of thin films. Phys. Rev. B. 65, 085409-8.
Hoagland, R., G., Mitchell, T., E., Hirth, J., P., 2002. Kung H. On the strengthening effects of interfaces in multilayer fee metallic composites. Philos. Mag. A. 82, 643-664.
Huang, H., Spaepen, F., 2000. Tensile testing of free-standing Cu, Ag and Al thin films and Ag/Cu multilayers. Acta Mater. 48, 3261-3269.
Koehler, J., S., 1970. Attempt of design a strong solid. Phys. Rev. B. 2, 547-551.
Lai, W., S., Yang, M., J., 2007. Observation of largely enhanced hardness in nano-multilayers of the Ag–Nb system with positive enthalpy of formation. Appl. Phys. Lett. 90, 181917.

Laugier, M., Palmqvist T., 1987. Indentation toughness in WC-Co composites. J. Mater. Sci. Lett. 6, 897-900.
Liu, Y., Wu, W., Chen, Q., Q., 2012. Zhu S. L, An J. J, Wang Z. Study of the Focusing Properties of Laue Bent Crystal by Ray-Tracing. ACTA PHYSICA SINICA. 61 (17).
Li, Y., P., Zhang, G., P., Wang, W., Tan, J., Zhu, S., J., 2007. On interface strengthening ability in metallic multilayers. Scripta Mater. 57, 117-120.
Mara, N., A., Tamayo, T., Sergueeva, A., V., Zhang, X., Misra, A., Mukherjee, A., K., 2007. The effects of decreasing layer thickness on the high temperature mechanical behavior of Cu / Nb nanoscale multilayers. Thin Solid Films. 515, 3241-3245.
Mara, N., A., Misra, A., Hoagland, R., G., Sergueeva, A., V., Tamayo, T., Dickerson, P., Mukherjee, A., 2008. K. High-temperature mechanical behavior/microstructure correlation of Cu/Nb nanoscale multilayers. Mater. Sci Eng A. 493, 274-284.
Mara, N., A., Bhattacharyya, D., Dickerson, P., Hoagland, R., G., Misra, A., 2008. Deformability of ultrahigh strength 5nm Cu/Nb nanolayered composites. Appl. Phys Lett. 92, 231901.
Mardon, J., P., Garner, G., Beslu, P., Charquet, D., Senevat, J., Proceedings of the 1997. International Topical Meeting on LWR Fuel Performance. Portland, Oregon.
Misra, A., Verdier, M., Lu, Y., C., Kung, H., Mitchell, T., E., Nastasi, M., and Embury, J., D., 1998. Structure and mechanical properties of Cu-X (X=Nb,Cr,Ni) nanolayered composites. Scripta Mater. 39, 555-560.
Misra, A., Kung, H., Hammon, D., Hoagland, R., G., Nastasi, M., 2003. *Damage* mechanisms in nanolayered metallic composites. Int. J. Damage Mech. 12, 365-376.
Misra, A., Hirth, J., P., Hoagland, R., G., 2005. Length-scale-dependent deformation mechanisms in incoherent metallic multilayered composites. Acta Mater. 53, 4817-4824.
Misra, A., and Hoagland, R., G., 2007. Plastic flow stability of metallic nanolaminate composites J. Mater. Sci. 42, 1765-1771.
Mukherjee, A., K., 2002. An examination of the constitutive equation for elevated temperature plasticity. Mater. Sci. Eng. A. 322, 1-22.
Meyers, M., A., Mishra, A., Benson, D., J., 2006. Mechanical properties of nanocrystalline materials. Prog. Mater. Sci. 51, 427-556.
Monclus, M., A., Karlik, A., Callisti, M., Frutos, E., Llorca, J., Polcar, T., Molina-Aldareguía, J., M., 2014. Microstructure and mechanical properties of physical vapour deposited Cu/W nanoscale multilayers: Influence of layer thickness and temperature. Thin Solid Films. 571, 275-282.
Oliver, W., C., Pharr, G., M., 1992. An improved technique for determining hardness and elastic modulus using load and displacement sensing indetation experimentes. J. Mater. Res. 7, 1564-1583.
Phillips, M., A., Clemens, B., M., Nix, W., D., 2003. A model for dislocation behavior during deformation of Al/Al_3Sc (fcc/$L1_2$) metallic multilayers. Acta Mater. 51, 3157-3170.
Rao, S., I., Hazzledine, P., M., 2000. Atomistic simulations of dislocation-interface interactions in the Cu-Ni multilayer system. Philos. Mag. A. 80, 2011-2040.
Suzuki, S., Murakami, K., Takahashi, T., Proceedings of the 1994. International Topical Meeting on LWR Fuel Performance, West Palm Beach, Florida.
Tabor, D., 1951. Hardness of Metals. Clarendon Press, Oxford.
Wan, D., T., Meng, F., L., Zhou, Y., C., Bao, Y., W., Chen, J., X., 2008. Effect of grain size, notch width, and testingtemperature on the fracture toughness of $Ti_3Si(Al)C_2$ and Ti_3AlC_2 using the chevron-notched beam (CNB) method. J. Eur. Ceram. Soc. 28, 663-669.
Wang, Y., C., Misra, A., Hoagland, R., G., 2006. Fatigue properties of nanoscale Cu/Nb multilayers. Scripta Mater. 54, 1593-1598.
Was, G., S., Foecke, T., 1996. Deformation and fracture in microlaminates. Thin Solid Filmas. 286, 1-31.
Whitney, J., M., Browing, C., E., Hoogsteden, W., 1982. A Double Cantilever Bema Test for Characterizing Mode I Delamination of Composite Materials. J. Reinf. Plast. Compos. 1, 297-313.
Wen, S., P., Zong, R., L., Zeng, F., Gao, Y., Pan, F., 2007. Nanoindentation investigation of the mechanical behaviors of nanoscale Ag/Cu multilayers. J. Mater. Res. 22, 3423-3431.
Ye, T., Suo, Z., Evans, A., G., 1992. Thin film cracking and the roles of substrate and interface. Jr. Int. J. Solids. Structures. 29, 2639-2648.
Zhang, G., P., Volkert, C., A., Schwaiger, R., Wellner, P., Arzt, E., Kraft, O., 2006. Length-scale-controlled fatigue mechanisms in thin copper films. Acta Mater. 54, 3127-3139.
Zhang, G., P., Liu, Y., Wang, W., Tan, J., 2006. Experimental evidence of plastic deformation instability in nanoscalemultilayers. Appl. Phys. Lett. 88, 013105.
Zhang, J., Y., Niu, J., J., Zhang, X., Zhang, P., Zhang, G., J., Sun, J., 2012. Tailoring nanostructured Cu/Cr multilayer films with enhanced hardness and tunable modulus. Mater. Sci. Eng. A. 543, 139-144.
Zhu, X., F., Li, Y., P., Zhang, G., P., Tan, J., Liu, Y., 2008. Understanding nanoscale damage at a crack tip of multilayered metallic composites. Appl. Phys. Lett. 92, 161905.